

# Baryon Asymmetry of the Universe in the $\nu$ MSM

---

**Laurent Canetti and Mikhail Shaposhnikov**

*Institut de Théorie des Phénomènes Physiques,  
École Polytechnique Fédérale de Lausanne,  
CH-1015 Lausanne, Switzerland*

*E-mail:* [Laurent.Canetti@epfl.ch](mailto:Laurent.Canetti@epfl.ch), [Mikhail.Shaposhnikov@epfl.ch](mailto:Mikhail.Shaposhnikov@epfl.ch)

**ABSTRACT:** We perform a detailed analysis of baryon asymmetry generation in the  $\nu$ MSM (an extension of the Standard Model by three singlet Majorana fermions with masses below the Fermi scale). Fixing a number of parameters of the  $\nu$ MSM by the neutrino oscillation data, we determine the remaining domain of the parameter space from the requirement of successful baryogenesis. We derive, in particular, the constraints on the mass splitting of a pair of singlet fermions, and on the strength of their coupling to ordinary leptons, essential for searches of these particles in rare decays of mesons and in beam-dump experiments with intensive proton beams.

---

## Contents

<b>1. Introduction</b>	<b>1</b>
<b>2. Basic equations</b>	<b>4</b>
2.1 Lagrangian and parameters	4
2.2 The framework	5
2.3 Analytical expression for baryon asymmetry	7
<b>3. Domain of the parameters leading to baryon asymmetry</b>	<b>8</b>
<b>4. Conclusions</b>	<b>12</b>
<b>A. The numerical method</b>	<b>12</b>
<b>B. Baryon asymmetry as a function of <math>\nu</math>MSM parameters</b>	<b>15</b>
<b>C. CP phases and maximal baryon asymmetry</b>	<b>18</b>

---

## 1. Introduction

There are many ways the baryon asymmetry of the Universe (BAU) could have arisen. They differ from each other by the nature of baryon and lepton number non-conservation, CP-violation and by the manner a departure from thermal equilibrium is realised. For practical purposes it is important to distinguish between the scenarios which can or cannot be *experimentally tested*. By experimentally testable we mean those in which particle physics experiments (limiting the time-scale by the existing accelerators including the LHC, and by the ILC, CLIC or an  $e\gamma$  collider for the future) could potentially determine *all* parameters of the theory, necessary for theoretical computation of the *amplitude* and of the *sign* of the baryon asymmetry of the Universe<sup>1</sup>.

The number of *experimentally testable* scenarios is quite limited. Basically, all the mechanisms for baryogenesis, which use new physics at energies much higher than the Fermi scale do not fall in this category. For example, the GUT baryogenesis (for a review see [1]) is not testable, as it includes superheavy particles with masses of the order of  $\mathcal{O}(10^{16})$  GeV, the direct search of which is impossible. The thermal leptogenesis (for a review see [2]) is only partially testable. It did pass the important tests coming from the observed neutrino masses and mixings, but the prediction of the baryon asymmetry in it

---

<sup>1</sup>Of course, the requirement of testability is not a “physical” one in a sense that the Nature is not obliged to be nice to us.

depends on CP-breaking phases which cannot be measured in low energy experiments, as the typical mass of the superheavy Majorana leptons is  $\mathcal{O}(10^{10})$  GeV - too high to allow their creation in laboratory.

If new particles, responsible for BAU, are in the reach of existing or future colliders, the baryogenesis mechanism has more chances to be testable. One of the examples is the resonant leptogenesis of [3, 4]. It uses essentially the same physics as thermal leptogenesis, but relies on a possible degeneracy of heavy Majorana leptons. This allows to shift their masses to the region accessible by the LHC or linear colliders, but still larger than the electroweak scale. Though the interactions of one of the Majorana leptons, relevant for BAU, are too weak to lead to its discovery at colliders [5], two other heavy leptons can be found and a peculiar flavour structure of their interactions can provide the “smoking gun” signature of the resonant leptogenesis [3, 6]<sup>2</sup>.

Yet another example is the electroweak baryogenesis (for reviews see [7, 8, 9]) where the source of baryon number non-conservation is the rapid high-temperature anomalous processes with fermion number violation [10], and departures from thermal equilibrium are due to strongly first order electroweak phase transition [11, 12]. The electroweak baryogenesis requires an extension of the Standard Model *right above* the electroweak scale, leading to specific predictions for LHC and ILC (see [13, 14] for recent discussions).

The baryogenesis can also occur due to new particles with the masses *considerably smaller* than the Fermi scale. An example (actually, the the only one, known to the authors) is associated with the minimal extension of the Standard Model (SM) in neutrino sector - the  $\nu$ MSM [15, 16]. In this model one adds to the SM three singlet Majorana leptons with masses smaller than the electroweak scale and uses the standard sea-saw Lagrangian, though with the completely different choice parameters (for a review see [17]). The lightest neutral singlet lepton with the mass in  $\mathcal{O}(10)$  keV region can be the dark matter (DM) candidate; the other two with masses  $M \sim \mathcal{O}(1)$  GeV would then generate the baryon asymmetry of the Universe. The Higgs boson with non-minimal coupling to gravity in the same model can play the role of the inflaton and make the Universe flat, homogeneous and isotropic, producing cosmological perturbations leading to structure formation [18]. The fact that so modest and natural modification of the SM can address at once many problems which the SM cannot solve (neutrino masses and oscillations, dark matter, baryon asymmetry of the Universe and inflation) forces us to take it seriously and study in detail the predictions of  $\nu$ MSM, which can be used as a guideline for experimental searches for new particles it contains<sup>3</sup>.

The astrophysical observations coming from X-ray satellites tell that the coupling of the lightest (DM) singlet fermion  $N_1$  to active neutrinos is so small that it practically does not contribute to the see-saw formula [24]. This means that two other singlet fermions of the  $\nu$ MSM  $N_{2,3}$  must be able to explain *simultaneously* the pattern of neutrino masses

---

<sup>2</sup>We thank A. Pilaftsis for discussion of this point.

<sup>3</sup>Further extensions of the  $\nu$ MSM are surely possible. See [19, 20, 21, 22] for discussion of the model with extra scalar singlet and [23] for analysis of the model with higher-dimensional operators added. Of course, the predictions of these models are less certain than those of the  $\nu$ MSM.

and oscillations and lead to baryogenesis. The parameter counting goes as follows<sup>4</sup>. Out of 11 new parameters of the model 7 can be (potentially) measured in experiments with active neutrino flavours only (these are 3 mixing angles, one Dirac CP-violating phase, one Majorana phase, and 2 active neutrino masses, the lightest one is massless in this approximation). The other 4 can be conveniently chosen as  $M = \frac{1}{2}(M_1 + M_2)$  – the average Majorana mass,  $\Delta M_M = \frac{1}{2}(M_1 - M_2)$  – the mass splitting,  $\epsilon < 1$  – the ratio of the strengths of the couplings of  $N_2$  versus  $N_3$  to leptons, and finally  $\eta$  – an extra CP-violating Majorana phase. Whether  $N_{2,3}$  can be found experimentally depends crucially on 2 parameters – their mass and  $\epsilon$  [25]. The main aim of the present paper is to find the constraints on these two parameters from the requirement of successful baryogenesis.

The idea that a pair of light (with masses in GeV region) and almost degenerate Majorana leptons can result in baryogenesis through their oscillations goes back to ref. [26]. The equations governing baryogenesis in the  $\nu$ MSM, incorporating the relevant physical effects (singlet fermion oscillations, transfer of fermion number from singlet species to active leptons and back, etc.) were formulated in [16], where it was shown that the  $\nu$ MSM can lead to baryon asymmetry of the Universe and give a dark matter candidate, being perfectly consistent with the data on neutrino oscillations. In that paper a perturbative solution to the kinetic equations was found, valid in a certain part of the parameter space<sup>5</sup>. A semi-quantitative analytic consideration of baryogenesis in the  $\nu$ MSM beyond perturbation theory has been carried out in [27], where different essential time scales were analysed, and the generic dependence of the baryon asymmetry on some of the  $\nu$ MSM parameters was elucidated.

An accurate prediction for properties of singlet fermions call, however, for a complete exploration of the parameter space and thus for a numerical solution of the kinetic equations, without any assumptions about hierarchies of different time scales, made in analytical computations. To identify the parameter-space allowing for baryogenesis, we calculate the baryon asymmetry as a function of the constants of the  $\nu$ MSM as follows. We fix the parameters of the neutrino mass matrix ( $\theta_{12}$ ,  $\theta_{23}$ ,  $\theta_{13}$ ,  $\Delta m_{atm}^2$ , and  $\Delta m_{sol}^2$ ) to their experimental values. For any given mass  $M$ , mass difference  $\Delta M_M$  and  $\epsilon$  we determine the maximum of BAU as a function of unknown CP-violating phases and require that this value is larger than the observed one. This allows to fix the 3-dimensional domain of parameters ( $M$ ,  $\Delta M_M$ ,  $\epsilon$ ), most relevant for experimental searches of  $N_{2,3}$ .

This paper is organised as follows. In Section 2 we summarise the basic properties of the model and formulate the kinetic equations for baryogenesis. In Section 3 we describe the results of numerical analysis. The Section 4 is conclusions. A number of appendixes contain details of the numerical procedure. In fact, a direct numerical solution of the kinetic equations poses a technical problem, as the corresponding differential equations belongs to the so-called “stiff” type. The reason is the existence of the many vastly different time scales, associated with oscillations and with relaxations of distinct types of deviations from

---

<sup>4</sup>From now on we omit the DM singlet fermion from consideration, as irrelevant for active neutrino masses and for baryogenesis.

<sup>5</sup>It is required that both  $N_{2,3}$  are out of equilibrium at the sphaleron freezing temperature  $T_{sph}$  and that the rate of  $N_{2,3}$  oscillations exceeds the rate of the Universe expansion at  $T_{sph}$ .

thermal equilibrium. In appendix A we transform the kinetic equations, governing the evolution of the system into a convenient form, which allows to elucidate the hierarchy of the relevant time-scales (the rate of the singlet fermion oscillations, coherence loss, transfer of leptonic number from sterile to active species, back reaction, leptonic flavour non-conservation, etc) and describe an effective way to solve them numerically. In appendix B we discuss the dependence of baryon asymmetry on the parameters  $M$ ,  $\Delta M_M$  and  $\epsilon$ , and its time evolution. In C we compute the maximal baryon asymmetry which can be created in  $\nu$ MSM.

## 2. Basic equations

This chapter is a brief review of the baryogenesis in the  $\nu$ MSM. First, we will describe the model, then we will formulate the kinetic equations, and finally we present the results of perturbative computation of the asymmetry, to be compared with numerics later. We use the same notations as in [27].

### 2.1 Lagrangian and parameters

The part of the Lagrangian of the  $\nu$ MSM we are interested at can be written as:

$$\begin{aligned} \mathcal{L} = & i\bar{N}_I \partial_\mu \gamma^\mu N_I + \mathcal{F} \left( \frac{e^{-i\eta/2}}{\sqrt{\epsilon}} \bar{L}_2 N_2 + \sqrt{\epsilon} e^{i\eta/2} \bar{L}_3 N_3 \right) \tilde{\Phi} \\ & - M \bar{N}_2^c N_3 - \frac{\Delta M_M}{2} (\bar{N}_2^c N_2 + \bar{N}_3^c N_3) + h.c., \end{aligned} \quad (2.1)$$

where  $N_2$  and  $N_3$  are the singlet leptons and  $M \pm \Delta M_M$  their Majorana masses,  $\tilde{\Phi}_i = \epsilon_{ij} \Phi_j^*$  is the Higgs doublet and  $v = 174$  GeV its vacuum expectation value,  $\epsilon$  is the ratio between the strengths of the couplings of  $N_3$  and  $N_2$  ( $\epsilon < 1$  by convention) and  $\eta$  is a CP-violating phase as explained in the Introduction. The constant  $\mathcal{F}^2$  is expressed through active neutrino masses  $m_i$  as

$$\mathcal{F}^2 = \frac{M}{2v^2} \sum_i m_i. \quad (2.2)$$

The 6 out of the 11 new parameters of the model are explicitly written in the Lagrangian (2.1) ( $M$ ,  $\Delta M_M$ ,  $\epsilon$ ,  $\eta$  and  $m_i$ ). The other 5, related to the active neutrino mixing matrix, are hidden is  $L_2$  and  $L_3$  which are combination of  $L_e$ ,  $L_\mu$  and  $L_\tau$ , the lepton doublets. These parameters are 3 mixing angles  $\theta_{12}$ ,  $\theta_{13}$ ,  $\theta_{23}$ , one Dirac phase  $\phi$  and one Majorana phase. It will be denoted by  $\alpha$  for the normal active neutrinos mass hierarchy and  $\xi$  for the inverted one, see [28] for convention. The relations between  $L_{2,3}$  and the flavour eigenstates were found in [27], we present them here for  $\theta_{13} = 0$  and  $\theta_{23} = \frac{\pi}{4}$ , which is within the experimental error bars (for a review see [28]).

For the normal hierarchy we have:

$$\begin{aligned} L_2 = & +a_1 \frac{L_\mu - L_\tau}{\sqrt{2}} + a_2 L_e + a_3 \frac{L_\mu + L_\tau}{\sqrt{2}}, \\ L_3 = & -a_1 \frac{L_\mu - L_\tau}{\sqrt{2}} - a_2 L_e + a_3 \frac{L_\mu + L_\tau}{\sqrt{2}}, \end{aligned} \quad (2.3)$$

where the coefficients are :

$$\begin{aligned}
a_1 &= ie^{-i(\alpha+\phi)} \sin \varrho \cos \theta_{12} , \\
a_2 &= ie^{-i\alpha} \sin \varrho \sin \theta_{12} , \\
a_3 &= \cos \varrho , \\
\tan \varrho &= \sqrt{\frac{m_2}{m_3}} \simeq \left( \frac{\Delta m_{\text{sol}}^2}{\Delta m_{\text{atm}}^2} \right)^{\frac{1}{4}} \simeq 0.4 .
\end{aligned} \tag{2.4}$$

For the inverted hierarchy the expressions are similar :

$$\begin{aligned}
L_2 &= +ie^{-i\phi} b_1 \frac{L_\mu - L_\tau}{\sqrt{2}} + b_2 L_e , \\
L_3 &= -ie^{-i\phi} b_2^* \frac{L_\mu - L_\tau}{\sqrt{2}} + b_1^* L_e ,
\end{aligned} \tag{2.5}$$

with the coefficients :

$$\begin{aligned}
b_1 &= \frac{1}{\sqrt{2}} \left[ \cos \theta_{12} e^{-i\zeta} + i \sin \theta_{12} e^{+i\zeta} \right] , \\
b_2 &= \frac{1}{\sqrt{2}} \left[ \cos \theta_{12} e^{+i\zeta} + i \sin \theta_{12} e^{-i\zeta} \right] .
\end{aligned} \tag{2.6}$$

For the analysis of kinetic equations, it is convenient to define the Yukawa coupling matrix  $F_{\alpha I}$  between the singlet fermion and the lepton doublet in the following way:

$$\begin{aligned}
\sum_{\alpha} F_{\alpha 2} \bar{L}_{\alpha} &= \frac{i\mathcal{F}}{\sqrt{2}} \left( \frac{e^{-i\eta/2}}{\sqrt{\epsilon}} \bar{L}_2 - \sqrt{\epsilon} e^{i\eta/2} \bar{L}_3 \right) , \\
\sum_{\alpha} F_{\alpha 3} \bar{L}_{\alpha} &= \frac{\mathcal{F}}{\sqrt{2}} \left( \frac{e^{-i\eta/2}}{\sqrt{\epsilon}} \bar{L}_2 + \sqrt{\epsilon} e^{i\eta/2} \bar{L}_3 \right) ,
\end{aligned} \tag{2.7}$$

which corresponds to a basis where the singlet fermion Majorana mass matrix  $\mathcal{M}$  is diagonal and equals to:

$$\mathcal{M} = \begin{pmatrix} M - \Delta M_M & 0 \\ 0 & M + \Delta M_M \end{pmatrix}. \tag{2.8}$$

## 2.2 The framework

A convenient way to treat a system of interacting Majorana fermions and neutrinos is to use a density matrix  $\rho$  [29, 30, 31]. Since we consider 2 singlet fermions and 3 active neutrinos and their anti-particles,  $\rho$  is a  $10 \times 10$  matrix. For baryogenesis the temperatures are above the electroweak scale  $T_W \sim 100$  GeV, we also take  $M \ll T_W$ . In this case the matrix  $\rho$  can be simplified [16]: it can be described by 3 chemical potentials  $\mu_{\alpha}$  for active neutrino species and by two  $2 \times 2$  density matrices for the sterile neutrinos, one for positive helicity states,  $\rho_N$  and one for negative helicity states  $\bar{\rho}_N$ . The evolution of the

system satisfies the kinetic equations which take into account creation of singlet fermions, their oscillations, and generation of lepton asymmetries [16]. Introducing the CP-even and CP-odd deviations from thermal equilibrium:

$$\begin{aligned}\delta\rho_+ &= \frac{\rho_N + \bar{\rho}_N}{2} - \rho^{eq}, \\ \delta\rho_- &= \rho_N - \bar{\rho}_N,\end{aligned}\tag{2.9}$$

where  $\rho^{eq} = \exp(-\frac{p}{T})$  with  $p$  the momentum of the sterile neutrino [16], these kinetic equations are [16, 27]:

$$\begin{aligned}i\frac{d\delta\rho_+}{dt} &= [\text{Re } H_N^{int}, \delta\rho_+] - \frac{i}{2}\{\text{Re } \Gamma_N, \delta\rho_+\} + i\frac{T}{8}\sin\varphi\left(F^\dagger\mu F - F^T\mu F^*\right) \\ &\quad + \frac{i}{2}[\text{Im } H_N^{int}, \delta\rho_-] + \frac{1}{4}\{\text{Im } \Gamma_N, \delta\rho_-\},\end{aligned}\tag{2.10}$$

$$\begin{aligned}i\frac{d\delta\rho_-}{dt} &= [\text{Re } H_N^{int}, \delta\rho_-] - \frac{i}{2}\{\text{Re } \Gamma_N, \delta\rho_-\} + i\frac{T}{4}\sin\varphi\left(F^\dagger\mu F + F^T\mu F^*\right) \\ &\quad + 2i[\text{Im } H_N^{int}, \delta\rho_+] + \{\text{Im } \Gamma_N, \delta\rho_+\},\end{aligned}\tag{2.11}$$

$$\begin{aligned}i\frac{d\mu}{dt} &= \text{diag}\left[-\frac{i}{2}\{\Gamma_L, \mu\}\right. \\ &\quad \left.+ i\frac{T}{16}\sin\varphi\left(F(\delta\rho_- + 2\delta\rho_+)F^\dagger - F^*(\delta\rho_- - 2\delta\rho_+)F^T\right)\right].\end{aligned}\tag{2.12}$$

Here  $F_{\alpha I}$  is Yukawa coupling matrix introduced in the previous chapter,

$$\Gamma_N = \frac{T}{4}\sin\varphi F^\dagger F, \quad \Gamma_L = \frac{T}{4}\sin\varphi \text{Re}[FF^\dagger]\tag{2.13}$$

are the rates of creation of singlet and active fermions correspondingly, and the oscillation Hamiltonian is given by

$$H_N^{int} = \frac{T}{8}F^\dagger F + \frac{1}{T}\text{diag}\left[-M\Delta M_M, M\Delta M_M\right].\tag{2.14}$$

The expressions (2.13, 2.14) were found for temperatures above  $T_W$  in the symmetric phase of electroweak theory,  $\sin\varphi \simeq 0.02$  is related to the ratio of the absorptive to the real part of neutrino propagator in the medium [26, 16].

The kinetic equations are written in the so-called monochromatic approximation, which assumes that the different energy modes of singlet fermions are effectively decouple. This is true in our case, as the collisions between  $N_{2,3}$  can be surely neglected, and the problem is linear in terms of the density matrix for the singlet fermions<sup>6</sup>.

The equations (2.10,2.11,2.12), supplemented by initial conditions with no lepton asymmetry for the active leptons ( $\mu = 0$ ) and zero abundance for the singlet fermions ( $\delta\rho_+ = -\rho^{eq}$ ,  $\delta\rho_- = 0$ ) describe the evolution of active and sterile neutrinos from CP-symmetric initial state. The choice of the initial condition for the CP-even part of the

---

<sup>6</sup>In general, this is not the case for active neutrinos in core collapse supernova, where one needs to take into account neutrino-neutrino interactions, leading to non-linear effects [32, 33]. We thank E. Akhmedov and A. Smirnov for discussion of this point.

density matrix  $\delta\rho_+$  is motivated by the following facts. First, the  $\nu$ MSM interactions of singlet fermions are so weak that they are out of thermal equilibrium till temperature  $T_+$  which is close to the electroweak scale (see the estimates of  $T_+$  as a function of the parameters of the  $\nu$ MSM in [27]). Therefore, they are not produced at  $T > T_+$ . Second, in the minimal setup of the  $\nu$ MSM, where inflation occurs due to the Higgs boson [18], the initial conditions for the kinetic equations can be found. They coincide exactly with those formulated above [23]. Moreover, the dependence of the produced baryon asymmetry on the initial condition for the CP-even part of the density matrix is linear in  $\delta\rho_+$ . Even if the singlet leptons had relatively strong non- $\nu$ MSM interactions at high energy scale, their initial (for our kinetic equations) abundance will be in the interval  $-\rho^{eq} < \delta\rho_+ < 0$ . In other words, the produced baryon asymmetry for generic initial conditions for  $\delta\rho_+$  can only be smaller than what we found. So, the prediction of the domain of the parameters, where baryogenesis in the  $\nu$ MSM *is not possible*, and therefore, identification of the experimental goals for their search (Figs. 1 - 4) is robust. At the same time, if  $|\delta\rho_+| < \rho^{eq}$ , the region where baryogenesis in the  $\nu$ MSM *is possible* will decrease correspondingly.

An analytic solution to these equations in a particular limit, discussed in the following subsection, was found in [16]. The qualitative features of this system of kinetic equations have been explored in [27]. We will use them to compute numerically the baryon asymmetry of the Universe as a function of the  $\nu$ MSM parameters in Section 3. Note that the transfer of the lepton asymmetry to the baryon asymmetry because of sphalerons is not included into eqns. (2.10,2.11,2.12), this can be done analytically in a standard way (see, e.g. [34]).

### 2.3 Analytical expression for baryon asymmetry

The equations (2.10), (2.11) and (2.12) can be solved perturbatively for small Yukawa couplings, provided the following assumptions are satisfied [16]:

- (i) Singlet fermions are out of thermal equilibrium for all temperatures above the sphaleron freeze-out,  $\Gamma_N \cdot t_W < 1$  with  $\Gamma_N \simeq \sin\varphi \frac{T\mathcal{F}^2}{8\epsilon}$ ,  $t_W \simeq M_0/T_W^2$ , where  $M_0 = 7 \cdot 10^{17}$  GeV.
- (ii) The baryon asymmetry creation temperature  $T_L \simeq (4M\Delta M_M M_0)^{1/3}$  [26, 16] is much higher than the electroweak temperature,  $T_L > T_W$ .
- (iii) The mass difference between two singlet fermions is much larger than the mass difference between active neutrinos,  $\Delta M_M \gg 0.04$  eV for the normal hierarchy and  $\Delta M_M \gg 8 \cdot 10^{-4}$  eV for the inverted hierarchy.

The baryon to entropy ratio (the observed one is  $\frac{n_B}{s} \simeq (8.4 - 8.9) \cdot 10^{-11}$ ) is given by

$$\frac{n_B}{s} \simeq 7 \cdot 10^{-4} \text{Tr}(\delta\rho_-)|_{T_W} , \quad (2.15)$$

where  $Tr(\delta\rho_-)|_{T_W}$  can be found in [16] and can be conveniently parametrised as

$$Tr(\delta\rho_-)|_{T_W} \simeq 36 \cdot \delta_{CP} \cdot \left( \frac{\sin \varphi \mathcal{F}^2 M_0}{8 \epsilon T_W} \right)^3 \cdot \left( \frac{T_W^3}{4M\Delta M_M M_0} \right)^{2/3}, \quad (2.16)$$

$$\delta_{CP} = \frac{2\epsilon^3}{\mathcal{F}^6} \sum_{I,\alpha} |F_{\alpha I}|^2 \text{Im}[F_{\alpha 3}[F^\dagger F]_{32} F_{2\alpha}^\dagger]. \quad (2.17)$$

Due to the conditions (i) and (ii), the first and second brackets respectively are always smaller than 1. This formula was used recently to compute the baryon asymmetry of the Universe in the  $\nu$ MSM, where CP-violation is solely originated from the CP violation in the mixing matrix of active neutrinos (i.e. for  $\eta = 0$ ) in [35].

Qualitatively, if  $\Gamma_N \cdot t_W \gg 1$ , the singlet fermions equilibrate, and dilute the baryon asymmetry. If  $T_L \ll T_W$ , the oscillations of singlet leptons had no time to develop and the creation of baryon asymmetry is strongly suppressed [27]. In other words, the maximal asymmetry is generated when  $\Gamma_N \cdot t_W \sim 1$  and  $T_L \sim T_W$  simultaneously.

In general case, the conditions (i)- (iii) are not satisfied, and numerical solution of the kinetic equations is necessary. The results of this analysis are presented in the next Section.

### 3. Domain of the parameters leading to baryon asymmetry

In this chapter, we determine the 3-dimensional domain of the parameters  $\epsilon$ ,  $M$  and  $\Delta M_M$  that can lead to the observed baryon asymmetry. It is found in the following way. The active neutrino mass matrix parameters are fixed to be

$$\begin{aligned} \sin \theta_{12} &= \sqrt{0.3}, \quad \theta_{13} = 0, \quad \theta_{23} = \frac{\pi}{4}, \\ m_2 &= \sqrt{\Delta m_{sol}^2} = 9 \text{ meV}, \quad m_3 = \sqrt{\Delta m_{atm}^2} = 50 \text{ meV}, \end{aligned} \quad (3.1)$$

for the normal hierarchy and

$$m_2 = m_3 = \sqrt{\Delta m_{atm}^2}, \quad (3.2)$$

for the inverted hierarchy. The variation of the parameters in (3.1,3.2) within experimental error bars (shown, for instance, in [28]) does not lead to any significant changes in the admitted parameter range. The unknown CP-violating phases are chosen in such a way that baryon asymmetry is maximised (see appendix C). They are close to the values given below,

$$\eta \simeq \phi \simeq \frac{\pi}{2}, \quad \alpha \simeq \frac{\pi}{2}, \quad \xi \simeq \frac{\pi}{4}, \quad (3.3)$$

which corresponds to the following Yukawa couplings ratio:

$$|F_{e2}|^2 : |F_{\mu 2}|^2 : |F_{\tau 2}|^2 \simeq 1 : 11 : 11, \quad (3.4)$$

for the normal hierarchy and

$$|F_{e2}|^2 : |F_{\mu 2}|^2 : |F_{\tau 2}|^2 \simeq 48 : 1 : 1, \quad (3.5)$$

for the inverted hierarchy. The second set corresponds to the model I of [25] and the first set is somewhat between the models II and III, described in [25]. The sphaleron freezing temperature is set at  $T_W = 140$  GeV corresponding to the Higgs mass  $m_H = 125$  GeV [34]. We have also done the computations for  $T_W = 170$  GeV which correspond to  $m_H = 200$  GeV, but the results are very close to the case  $T_W = 140$  GeV.

With this set of parameters the kinetic equations (2.10), (2.11) and (2.12) are solved numerically with the methods described in appendix A. The admissible domain of the parameters is determined from the condition  $n_B/s|_{theoretical} > n_B/s|_{observed}$ . For masses above  $\sim 10$  GeV the computation should not be trusted, as the kinetic equations are only valid in the limit  $M \ll T_W$ . We expect that the admitted region of the singlet fermion masses in the  $\nu$ MSM closes up at  $M \sim M_W$  [27]. A number of intermediate results, such as dependence of baryon asymmetry on  $\epsilon$ ,  $M$  and  $\Delta M_M$ , and its time dependence, can be found in appendix B.

In the left panel of Fig. 1 we present the projection of the allowed region to the  $\epsilon - M$  plane for both neutrino mass hierarchies. Here, for every  $\epsilon$  and  $M$  the asymmetry is extremised with respect to  $\Delta M_M$ ; in the interior region the asymmetry is greater than the observed one, the boundary corresponds to  $n_B/s|_{theoretical} = n_B/s|_{observed}$ . The baryon asymmetry generation is possible for very light singlet fermions,  $M \simeq 10$  MeV for the normal hierarchy and  $M \simeq 1$  MeV for the inverted one. They correspond to small  $\epsilon \sim \text{few} \times 10^{-4}$ .

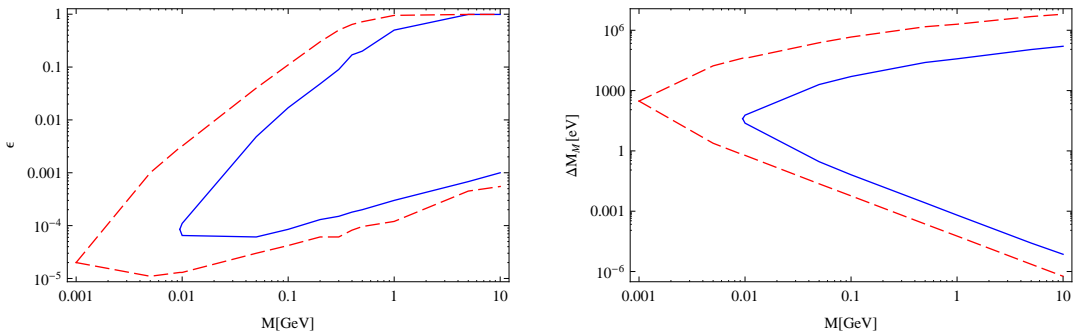


**Figure 1:** Values of  $\epsilon - M$  (left panel) and  $\Delta M_M - M$  (right panel) that leads to the observed baryon asymmetry for the normal hierarchy (blue - solid line) and for the inverted hierarchy (red - dashed line).

The right panel of Fig. 1 gives a projection of our domain to the  $\Delta M_M - M$  plane, which is derived in the similar way (asymmetry is now extremised with respect to  $\epsilon$  at fixed  $\Delta M_M$  and  $M$ ). The admitted mass difference ranges from a fraction of eV to MeV, depending on the singlet fermion mass.

In Fig. 2 we present yet other projections to the  $\Delta M_M - \epsilon$  plane for several singlet fermion masses and two different types of the hierarchies. In general, for larger masses the amount of the parameter space where baryogenesis happens is larger. Also, the inverted hierarchy has more parameter space than the normal one.

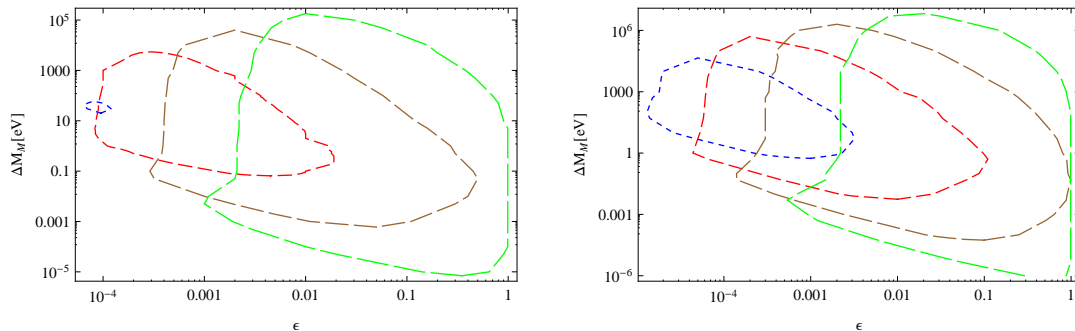


**Figure 2:** Values of  $\Delta M_M$  and  $\epsilon$  that leads to the observed baryon asymmetry for different singlet fermion masses,  $M = 10, 100$  MeV, 1, and 10 GeV. The blue (shortest dashed) line corresponds to  $M = 10$  MeV, red (short dashed) - to  $M = 100$  MeV, brown (long dashed) -  $M = 1$  GeV and green (longest dashed) to  $M = 10$  GeV. Left panel - normal hierarchy, right panel - inverted hierarchy.

For most important parameters for experimental searches of the singlet fermions are their mass and  $\epsilon$ , which determines the strength of the coupling of  $N_{2,3}$  to ordinary leptons. Usually it is expressed through the mixing angle  $U^2$  between ordinary and singlet leptons (we take a sum over mixing angles with all active neutrino flavours, for an exact definition see [25]). For small  $\epsilon$ ,

$$U^2 = \frac{\sum m_i}{4M\epsilon}. \quad (3.6)$$

The region, where baryogenesis is possible in  $U^2 - M$  plane is shown in Fig. 3, which is the main result of this paper<sup>7</sup>. It is derived from Fig. 1 with the use of (3.6). We also plot there the exclusion regions coming from different experiments such as BEBC [36], CHARM [37], and NuTeV [38] and CERN PS191 experiment [39, 40] (see also discussion of different experiments in [41]). For the case of normal hierarchy, only CERN PS191 have significantly entered into cosmologically interesting part of the parameter space of the  $\nu$ MMS, situated below the mass of the kaon. If the hierarchy is inverted, there are some constraints even for higher  $N$  masses. The lower constraint on  $U^2$ , coming from baryon asymmetry of the Universe, is somewhat stronger than the “see-saw” constraint. In Fig. 4 we present the expected life-time of the singlet fermions in an experimentally interesting region  $M < 2$  GeV.

A detailed discussion of possible experiments and signatures of neutral leptons leading to BAU generation in the  $\nu$ MMS can be found in [25]. For the reader convenience, we summarise below the main conclusions of this work.

Several distinct strategies can be used for the experimental search of these particles. The first one is related to  $N$  production ( $U^2$  effect). The singlet fermions participate in all the reactions the ordinary neutrinos do with a probability suppressed roughly by a factor  $U^2$ . Since they are massive, the kinematics of, say, two body decays  $K^\pm \rightarrow \mu^\pm N$ ,

<sup>7</sup>These figures supersede other similar plots which appeared previously in a number of works [25, 17] and in conference proceeding.

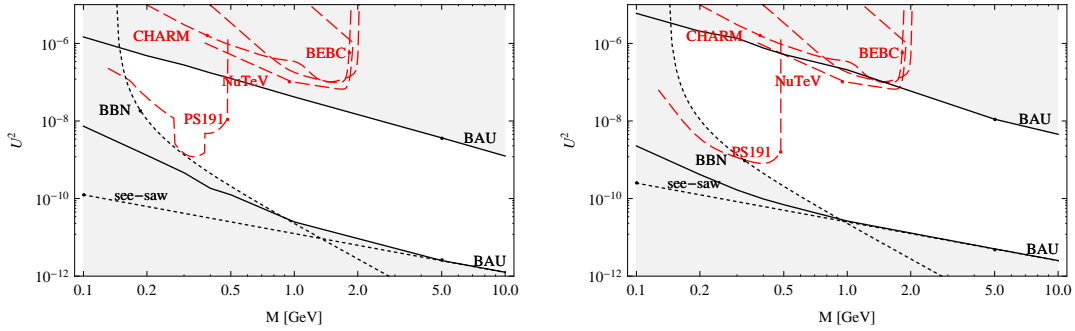


**Figure 3:** Constraints on  $U^2$  coming from the baryon asymmetry of the Universe (solid lines), from the see-saw formula (dotted line) and from the big bang nucleosynthesis (dotted line). Experimental searched regions are in red - dashed lines. Left panel - normal hierarchy, right panel - inverted hierarchy.

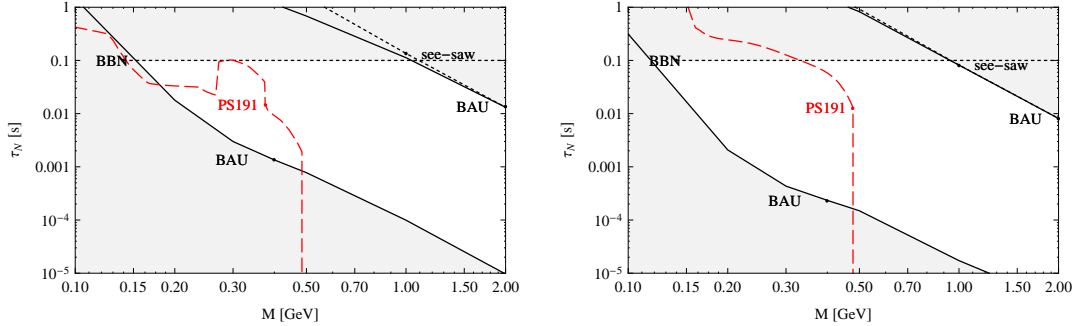


**Figure 4:** Constraints on the lifetime  $\tau_N$  coming from the baryon asymmetry of the Universe (solid lines), from the see-saw formula (dotted line) and from the big bang nucleosynthesis (dotted line). Experimental constraints from PS 191 are shown in red - dashed lines. Left panel - normal hierarchy, right panel - inverted hierarchy.

$K^\pm \rightarrow e^\pm N$  or three-body decays  $K_{L,S} \rightarrow \pi^\pm + e^\mp + N_{2,3}$  changes when  $N_{2,3}$  is replaced by an ordinary neutrino. Therefore, the study of *kinematics* of rare  $K$ ,  $D$ , and  $B$  meson decays can constrain the strength of the coupling of heavy leptons. The precise study of kinematics of rare meson decays is possible in  $\Phi$  (like KLOE), charm, and B factories, or in experiments with kaons where their initial 4-momentum is well known (like NA48, NA62 or E787 experiments).

The second strategy is to use the proton beam dump ( $U^4$  effect). As a first step, the proton beam heating the fixed target creates  $K$ ,  $D$  or  $B$  mesons, which decay and produce  $N_{2,3}$ . The second step is a search for decays of  $N$  in a near detector, looking for the processes “nothing”  $\rightarrow$  leptons and hadrons. To this end, quite a number of already existing or planned neutrino facilities (related, e.g., to CERN SPS, MiniBooNE, MINOS, J-PARC or LBNE at Fermilab), complemented by a near *dedicated* detector can be utilised.

For the mass interval  $M < M_K$ , both strategies can be used. If  $m_K < M < m_D$ , the

search for the missing energy signal, potentially possible at beauty, charm, and  $\tau$  factories, is unlikely to gain the necessary statistics and is impossible at hadronic machines like the LHC. Thus, the search for decays of neutral fermions is the most effective opportunity. The dedicated experiments on the basis of the proton beam NuMI or NuTeV at FNAL, SPS at CERN, or J-PARC can touch a very interesting parameter range for  $M < 1.8$  GeV. Experiments like NuSOng [42] and HiResM $\nu$  [43] should be able to enter in a cosmologically interesting region for masses and mixing angles of singlet fermions.

Going above  $D$ -meson but still below  $B$ -meson thresholds is very hard if not impossible with the present or planned proton machines or B-factories. To enter into a cosmologically interesting parameter space would require the increase in the present intensity of, say, CERN SPS beam by two orders of magnitude or to produce and study the kinematics of more than  $10^{10}$  B-mesons. For  $M$  above the beauty threshold  $\simeq 5$  GeV the baryogenesis in the  $\nu$ MSM becomes untestable.

## 4. Conclusions

In this paper we found the 3-dimensional domain of  $\nu$ MSM parameters ( $M$ ,  $\Delta M_M$ ,  $\epsilon$ ) that may lead to observed baryon asymmetry of the Universe. It ranges from the singlet fermion masses in MeV region to tens of GeV and from mass differences from a fraction of eV to MeV. Thus, baryogenesis is a generic consequence of the  $\nu$ MSM with nearly degenerate Majorana fermions. Our results can be used to determine an ultimate goal for searches for cosmologically interesting heavy neutral leptons, responsible for neutrino masses and oscillations, and for baryon asymmetry of the Universe.

The analysis of our work can be improved in several aspects. In particular, the kinetic equations we used are only approximate. They are dealing with a typical particle in the plasma with momentum  $\sim T$ . Clearly, the exact kinetic equations (to be derived yet) must have integro-differential character. We also did not take into account the mass corrections  $\mathcal{O}\left(\frac{M_M^2}{T^2}\right)$  and  $\mathcal{O}\left(\frac{M}{T^2}\right)$ . We postpone, however, the study of these effects till the moment when the singlet fermions are discovered.

## Acknowledgements

This work was supported in part by the Swiss National Science Foundation. We thank Takehiko Asaka and Dmitry Gorbunov for reading of the manuscript and for useful comments.

## A. The numerical method

The straightforward numerical solution of equations (2.10), (2.11) and (2.12) causes no problems for quite a wide range of the parameters of the  $\nu$ MSM. However, in some corners of the parameter space, where the damping is strong and/or oscillations are very rapid, it is faced with a number of difficulties. Due to simultaneous presence of many different time scales, related to damping of various quantum numbers and due to oscillations between

singlet fermions, the corresponding differential equations belongs to the so-called “stiff” type. For example, for typical parameters  $T_W \simeq 100$  GeV,  $M = 1$  GeV  $\Delta M_M = 10^{-6}$  GeV and  $\epsilon = 0.1$ , the oscillation rate  $\Delta E \simeq \frac{2M\Delta M_M}{T} = 2 \cdot 10^{-8}$  GeV is some 7 orders of magnitude larger than the rate of the singlet fermion creation,  $\Gamma_N \simeq \sin \varphi \frac{T}{8\epsilon} \mathcal{F}^2 = 2 \cdot 10^{-15}$  GeV. So, to solve kinetic equations numerically we will use a method which is very similar to the one developed in the Appendix A of Ref. [44]. The basic idea is to determine the damping and oscillation rates at any given moment of time and then disentangle the kinetic evolution accordingly. This is explained in detail below.

The system of equations (2.10), (2.11) and (2.12) can be rewritten in the form

$$-\frac{1}{i} \frac{d\psi}{dt} = \mathcal{H}\psi, \quad (\text{A.1})$$

where  $\psi$  is a real vector of dimensionality 11, which includes all unknowns, namely  $2 \times 4$  real functions determining density matrices for singlet fermions,  $\delta\rho_+$  and  $\delta\rho_-$ , and 3 chemical potentials for active leptonic asymmetries  $\mu_\alpha$ . The  $11 \times 11$  complex (but not Hermitian) matrix  $\mathcal{H}$  can be called effective Hamiltonian. The (complex, in general) eigenvalues of  $\mathcal{H}$  at some moment of time  $t$  give the instant relaxation and oscillation rates in the system.

Let us look for solutions of equation (A.1) in the form:

$$\psi(t) = e(t)E(t)\psi_0(t), \quad (\text{A.2})$$

where  $\psi_0(t)$  is some vector, and  $e(t)$  is a matrix build from the eigenvectors of the matrix  $\mathcal{H}$ :

$$\mathcal{H}e = ep, \quad (\text{A.3})$$

where  $p$  is a diagonal matrix, constructed from eigenvalues of  $\mathcal{H}$  and the matrix  $E(t)$  is defined by:

$$E(t) = \exp\left(-i \int_0^t dt' p(t')\right). \quad (\text{A.4})$$

In this way the rapidly oscillating or exponentially damped behaviour of  $\psi(t)$  is factored out, and  $\psi_0(t)$  is slowly varying. Now we will derive a convenient form of equation for  $\psi_0(t)$ .

Let us denote the eigenvectors of  $\mathcal{H}$  by  $e_i$ . Then we have  $\mathcal{H}e_i = p_i e_i$  and  $e = (e_1, e_2, \dots)$ . It is useful to introduce another set of the eigenvectors  $f_j$  defined by  $f_j \mathcal{H} = f_j q_j$  and introduce the matrix  $f$  as  $f = \begin{pmatrix} f_1 \\ f_2 \\ \dots \end{pmatrix}$ . The sets of eigenvalues  $q_j$  coincide with the set  $p_i$

up to permutation, since they are found from one and the same equation,  $\det(\mathcal{H} - p) = 0$  or  $\det(\mathcal{H} - q) = 0$ . If  $p_i \neq q_j$ , the vectors  $e_i$  and  $f_j$  are orthogonal,  $f_j e_i = 0$ . Therefore, the reshuffling of the set  $f_i$  can ensure that the matrices  $f$  and  $e$  satisfy  $fe = A$ , where  $A$  is a diagonal matrix. We can choose the normalisation of  $f$  and  $e$  in such a way that  $A = Identity$ , but we will keep it arbitrary in what follows.

Using the orthogonality of  $e$  and  $f$  one can get an equation for  $\psi_0(t)$ :

$$\frac{d\psi_0}{dt} = -(AE)^{-1} f \frac{de}{dt} E \psi_0, \quad (\text{A.5})$$

and the time evolution for the eigenvectors  $e(t)$  and the eigenvalues  $p(t)$ ,  $f(t)$ :

$$\frac{dp_i}{dt} = \frac{1}{A_{ii}} \left( f \frac{d\mathcal{H}}{dt} e \right)_{ii}, \quad (\text{A.6})$$

$$\frac{de}{dt} = e G, \quad (\text{A.7})$$

$$\frac{df}{dt} = -A G A^{-1} f, \quad (\text{A.8})$$

$$G_{ii} = 0, \quad G_{ij} = \frac{1}{(p_j - p_i) A_{ii}} \left( f \frac{d\mathcal{H}}{dt} e \right)_{ij}. \quad (\text{A.9})$$

The equation (A.5) is still not suitable for numerics due to explicit presence of exponentially small terms in the matrix  $E(t)$ , coming from imaginary parts of the eigenvalues and corresponding to strong damping (entering to thermal equilibrium of the corresponding processes). To avoid this kind of problem, we remove the imaginary part of the eigenvalues from the exponential by the change of variables:

$$\psi_0(t) = \exp \left( - \int_0^t dt' \text{Im}(p(t')) \right) \tilde{\psi}(t), \quad (\text{A.10})$$

$$\tilde{E}(t) = \exp \left( - i \int_0^t dt' \text{Re}(p(t')) \right), \quad (\text{A.11})$$

$$\psi(t) = e(t) \tilde{E}(t) \tilde{\psi}(t). \quad (\text{A.12})$$

The new equation for  $\tilde{\psi}(t)$  is:

$$\frac{d\tilde{\psi}}{dt} = \text{Im}(p) \tilde{\psi} - (A \tilde{E})^{-1} f \frac{de}{dt} \tilde{E} \tilde{\psi}. \quad (\text{A.13})$$

These equations were used for compute the behaviour of the density matrices and of the chemical potentials with the Wolfram Mathematica command NDSolve. It is convenient to use a dimensionless variable  $z$ , related to temperature as

$$z = \frac{h_0 \sin \varphi M_0}{4T} = \frac{h_0 \sin \varphi M_0}{4\sqrt{M_0/2t}}, \quad (\text{A.14})$$

with  $h_0 = 2 \times 10^{-14}$  and changing from 0 (initial state) to  $\sim 1$  (sphaleron freezing).

For some choice of the parameters the computation crashes and further refinements of the method were necessary.

First, if two of eigenvalues are equal to each other at some moment  $\tau_0$ , the equation (A.9) gets singular. To go around this problem, we continued the coordinate  $z$  to the complex plane, to go around the singularity:  $z = \tau + i \frac{a}{\cosh^2(b(\tau - \tau_0))}$ , where  $\tau$ ,  $a$  and  $b$  are some real parameters. The result must be independent of the specific choice of  $a$  and  $b$ , which we verified numerically.

Second, if the frequency of oscillations between two sterile neutrinos is very high, the numerical solution of (A.13) is extremely slow, as a very small time step size is required. At the same time, no asymmetry is produced in this regime, exactly due to the fact that

the oscillations are rapid [26, 16, 27]. Therefore, we introduced an artificial damping of oscillations, effectively averaging them to zero. This was done by multiplying  $\tilde{E}$  by  $\exp\left(-A\left(\int_0^t dt' \operatorname{Re}(p(t'))\right)^2\right)$ , where  $A$  is some real parameter. We verified numerically that this procedure indeed works.

## B. Baryon asymmetry as a function of $\nu$ MSM parameters

In this appendix we present some numerical results which clarify the dependence of the baryon asymmetry on the parameters of the model, and consider its time evolution. A comparison with a perturbative computation is also made.

For computations, we set the parameters related to the active neutrinos mass matrix as specified in eqns. (3.1,3.2, 3.3) and  $T_W = 100$  GeV.

In Fig. 5 we present the dependence of asymmetry on the mass  $M$  for some choices of other parameters ( $\epsilon$  and  $\Delta M_M$ ).

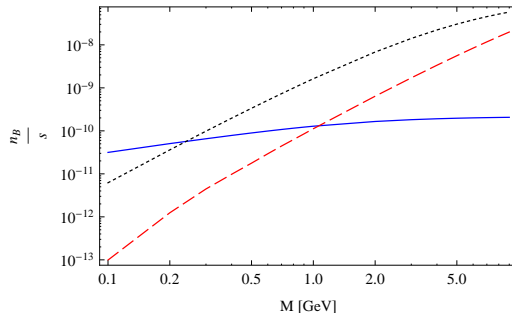


**Figure 5:** Baryon asymmetry as a function of  $M$  for  $\epsilon = 5 \cdot 10^{-4}$ ,  $\Delta M_M = 10^{-10}$  GeV in blue - solid line, for  $\epsilon = 0.5$ ,  $\Delta M_M = 10^{-10}$  GeV in red - dashed line and for  $\epsilon = 7 \cdot 10^{-2}$ ,  $\Delta M_M = 10^{-9}$  GeV in black - dotted line

In Fig. 6a, we show the dependence of the asymmetry on  $\Delta M_M$ , keeping  $M = 2$  GeV and  $\epsilon = 0.5$ , with latter two numbers chosen ad hoc. The upper line corresponds to the perturbative solution given by (2.16), and the lower one to numerical integration. These two curves are almost the same for  $\Delta M_M > 10^{-11}$  GeV. For smaller  $\Delta M_M$  the conditions (ii) and (iii) formulated in Section 2.3 are not valid any more. The asymmetry decreases for very small  $\Delta M_M$ , as the resonance has no time to develop.

In Fig. 6b we fix  $M = 2$  GeV and  $\Delta M_M = 10^{-6}$  GeV and vary  $\epsilon$ . The analytical perturbative solution is close to the numerical one for  $\epsilon > 0.01$ . This is what is expected: the condition (i) of Sect. 2.3 requires  $\epsilon \gtrsim 0.015$  to insure that the sterile neutrinos are out of thermal equilibrium. For smaller  $\epsilon$  the asymmetry decreases because the singlet fermions start to equilibrate.

In Fig. 6c we fix  $\epsilon = 0.5$ ,  $\Delta M_M = 10^{-6}$  GeV and vary  $M$ . The curves start to deviate from each other at large masses, where the condition (i) is not valid any longer.

In Fig. 7 we show the time evolution of different asymmetries for the following choice of parameters (for the normal hierarchy of neutrino masses). We take  $\epsilon = 0.015$ ,  $\Delta M_M = 10^{-8}$

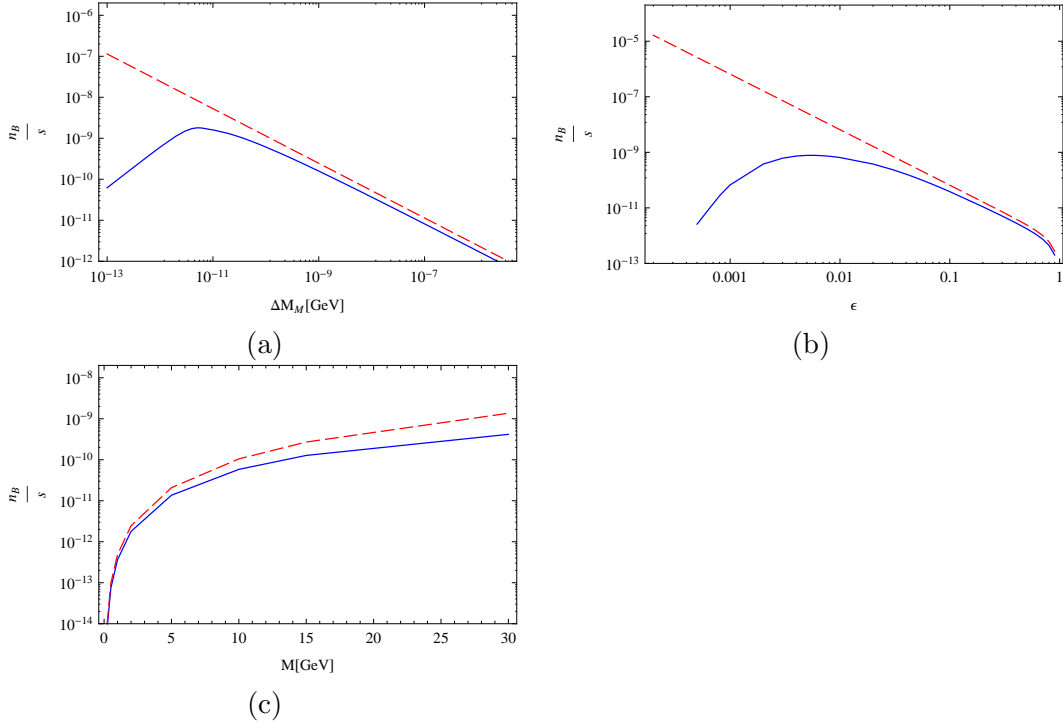


**Figure 6:** Lepton asymmetry in function of  $\Delta M_M$  (a),  $\epsilon$  (b),  $M$  (c), blue / solid line for numerical solution and red / dashed line for the analytic expression.

GeV and  $M = 1$  GeV, and consider evolution of the system till temperature  $T = 100$  GeV. These parameters are chosen in such a way that equilibration of singlet fermions occurs at  $T > T_W$  (so that  $\Gamma_N t_W > 1$ ). Therefore, one would expect that the asymmetry start to decrease after  $t \simeq 1/\Gamma_N$ . Also, for this choice  $T_L > T_W$  (see Sect. 2.3), indicating that the production of asymmetry in  $N_{2,3}$  occurs around the time corresponding to  $T_L$ . The time variable  $\tau$  used in these plots is defined in appendix A.

The asymmetries start to be produced around  $\tau \simeq 0.05$  (see Figs. 7a,b,c and below). The asymmetries in singlet fermion  $N_2$  is almost the same as in  $N_3$  (Fig. 7a). The asymmetries in  $\mu$  and  $\tau$  flavours are very close to each other (upper line in Fig. 7b). They start to decrease for  $\tau \gtrsim 0.5$ , which is the onset of damping (see below). The graph (7c) shows us that the asymmetry in the active sector is the same with the opposite sign as the one in the singlet sector.

In Fig. 8 we show the time evolution of the damping (left panel) and  $N_2 - N_3$  oscillation factors (right panel), appearing as exponentials in (A.10), for the relevant eigenvalue of the effective Hamiltonian  $\mathcal{H}$ :  $\int \text{Im}(p_{E_2}) dt$  and  $\int \text{Re}(p_{E_2}) dt$ . The numerical and analytical results of the first expression almost coincide for this particular choice of parameters, but not the real part due to our choice of CP-violating phases.

The oscillation exponent Fig. 8 (right panel) reaches 1 at  $\tau \simeq 0.05$ , which is the time when the asymmetries are produced on the graphs of Figure 7. The damping exponent Fig. 8 (left panel) approaches 1 at  $\tau \simeq 0.6$ , corresponding roughly to maximum of the

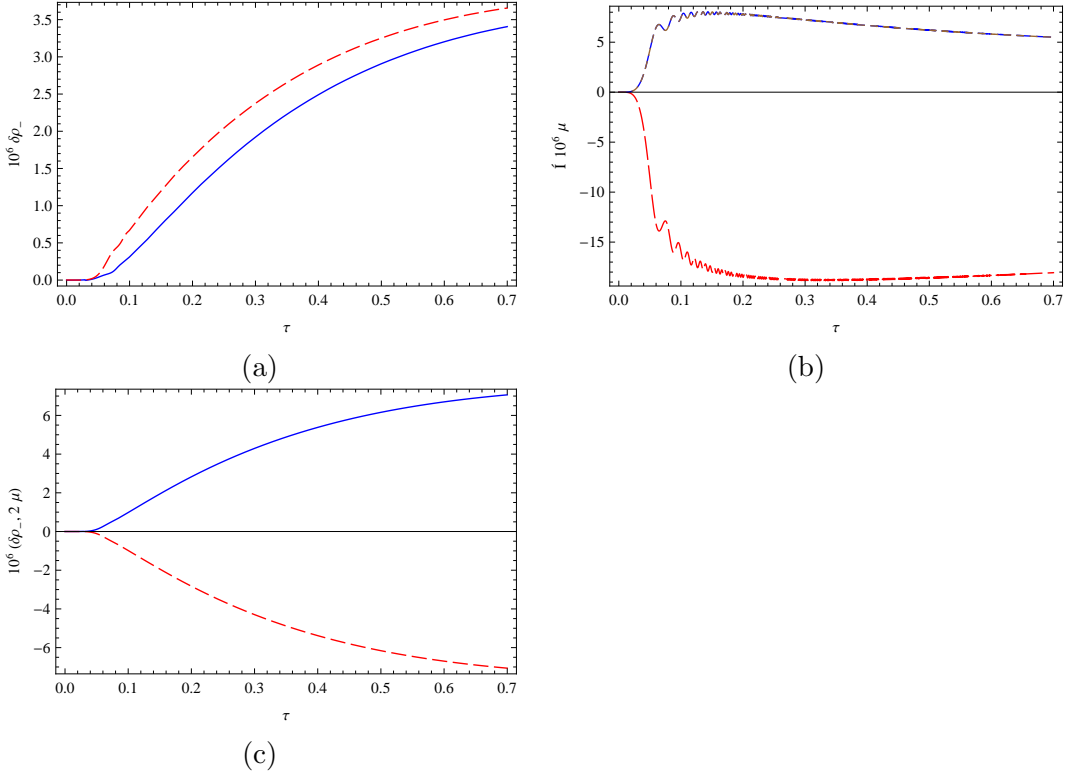


**Figure 7:** Asymmetries in the sterile sector (a) (blue - solid line for  $N_2$  and red - dashed line for  $N_3$ ), in the active sector (b) (red - long line for  $e$ , blue - short line for  $\mu$  and brown - dotted line for  $\tau$ ) and total asymmetries in both sector (c) (blue - solid line for the sterile sector and red - dashed line for the active sector).

asymmetries in Fig. 7b.

In general, the results of numerical integration are in accordance with the qualitative picture developed in [27].

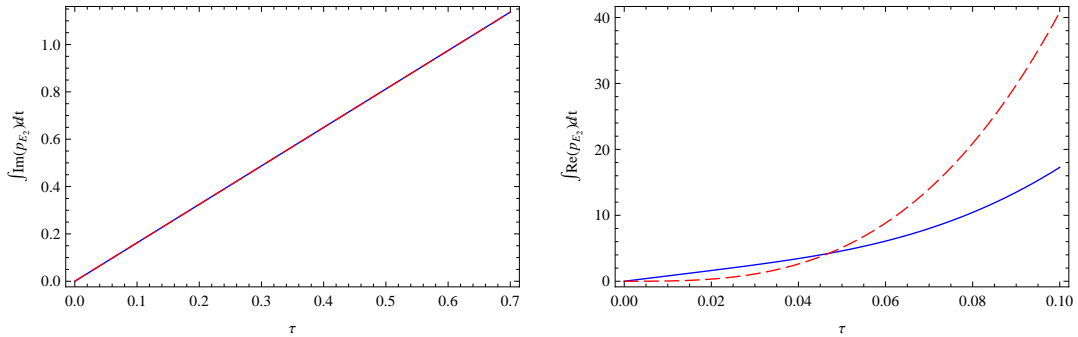


**Figure 8:** Time dependence of  $\int Im(p_{E_2}) dt$  (left) and of  $\int Re(p_{E_2}) dt$  (right). The numerical and analytical results are the same (blue - solid line for the numerical results and red - dotted line for the analytical solution).

### C. CP phases and maximal baryon asymmetry

Our procedure to find the parameter space of the  $\nu$ MSM leading to acceptable baryon asymmetry of the Universe implies the maximisation of the result with respect to three unknown phases  $\eta, \phi$  and  $\alpha$  for normal hierarchy and  $\eta, \phi$  and  $\xi$  for inverted. With the choice of active neutrino mass parameters (3.1,3.2) the numerical analysis shows that it is achieved close to  $\eta = \phi = \alpha = \frac{\pi}{2}$  and  $\xi = \frac{\pi}{4}$ . (Note that for  $\theta_{13} = 0$  and  $\theta_{23} = \frac{\pi}{4}$  and parametrisation of active neutrino mixing matrix as in [28] the Dirac phase  $\phi$  plays no role for inverted hierarchy.)

In Fig. 9 we show the dependence of asymmetry on  $\phi$  for a typical choice of  $M$ ,  $\Delta M_M$ , and  $\epsilon$  (left panel, fixing  $\eta = \alpha = \frac{\pi}{2}$ ) and on  $\alpha$  (right panel, fixing  $\eta = \phi = \frac{\pi}{2}$ ). In Fig. 10 we show the dependence of asymmetry on  $\xi$  (fixing  $\eta = \alpha = \frac{\pi}{2}$ ) for the case of inverted hierarchy.

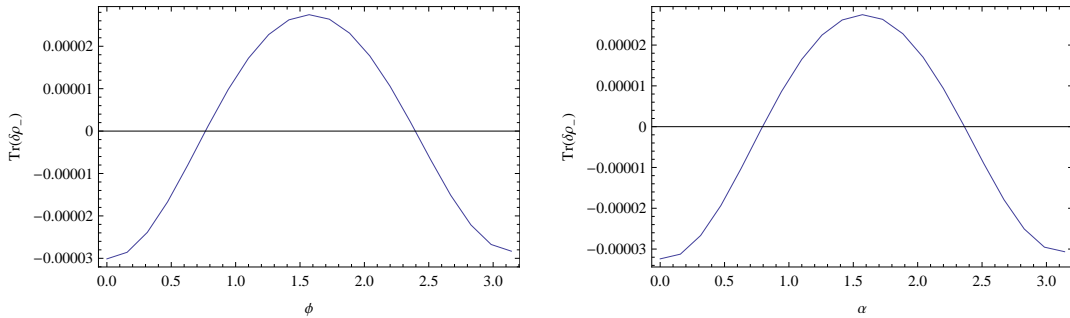


**Figure 9:** Lepton asymmetry as a function of  $\phi$  (left panel) and  $\alpha$  (right panel) for normal hierarchy.

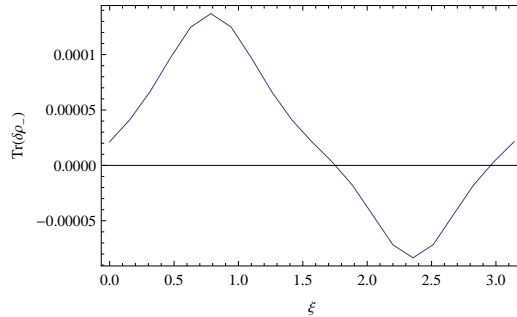


**Figure 10:** Lepton asymmetry as a function of  $\xi$  for inverted hierarchy.

The boundaries of the parameter space given in Sect. 3 correspond to the extremal choice of phases, found in this Appendix and to the observed baryon asymmetry. Below we will determine the values of  $M$ ,  $\Delta M_M$  and  $\epsilon$  which extremise asymmetry and find its maximum (using, again, the set of phases (3.3)).

As a guiding line for numerics, we can proceed first with the analytical estimate. In Fig. 11 we plot the dependence of  $\delta_{CP}$ , defined in (2.17) on  $\epsilon$ . In general, CP-violation is

larger in inverted hierarchy case and is maximal around  $\epsilon \simeq 0.5$ . Replacing the brackets in (2.16) by 1, we arrive to

$$\left. \frac{n_B}{s} \right|_{max} \simeq 1.5 \times 10^{-3} \quad (2.5 \times 10^{-4}) \quad (\text{C.1})$$

for inverted (normal) hierarchy. The asymmetry is expected to be maximal for

$$\frac{\sin \varphi \mathcal{F}^2 M_0}{8 \epsilon T_W} \sim 1, \quad \frac{T_W^3}{4M \Delta M_M M_0} \sim 1. \quad (\text{C.2})$$

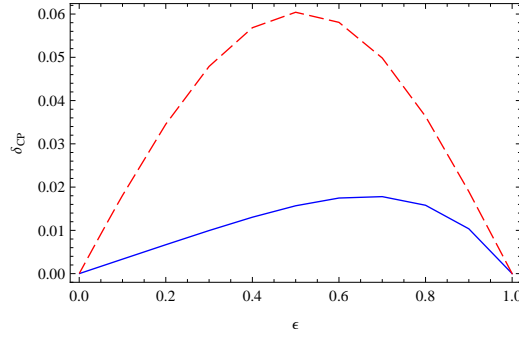


**Figure 11:**  $\delta_{CP}$  in function of  $\epsilon$  for the normal hierarchy (blue - solid line) and for the inverted hierarchy (red - dashed line).

These expectations can be verified by numerics. In Fig. 12 we show the dependence of the maximal asymmetry on the singlet fermion mass (for each choice of  $M$  and  $T_W$  we find the values of  $\epsilon$  and  $\Delta M_M$  that give the maximal asymmetry).

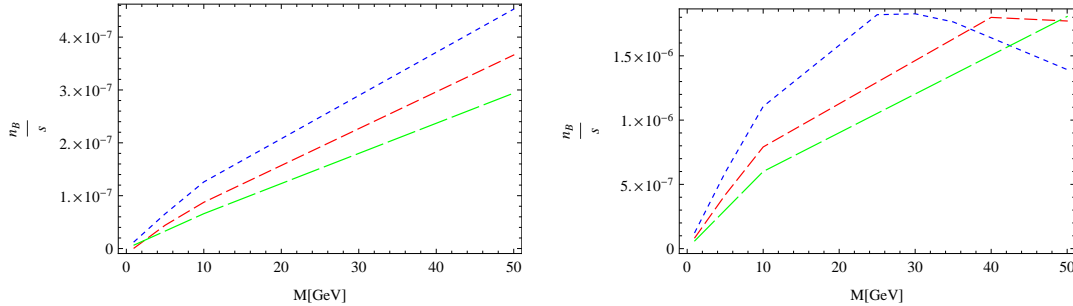


**Figure 12:** Maximal asymmetry as a function of  $M$  for  $T_W = 100$  GeV (blue - short dashed line),  $T_W = 150$  GeV (red - dashed line) and  $T_W = 200$  GeV (green - long dashed line). Left panel - normal hierarchy, right panel - inverted hierarchy.

In Fig. 13 we show for which  $\epsilon$  and  $\Delta M_M$  the asymmetry is maximised for different  $T_W$ , with the parameter along the curves being the mass  $M$ .

In Fig. 12, the maximal asymmetry for the normal hierarchy is reached for masses  $M$  bigger than 50 GeV. For the inverted hierarchy, the numerical computation of the

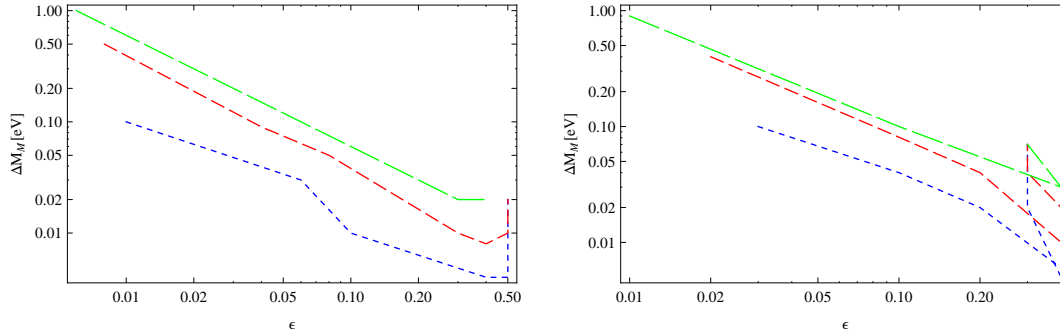


**Figure 13:** The parameters  $\epsilon$  and  $\Delta M_M$  corresponding to the maximal asymmetry for  $T_W = 100$  GeV (blue - short dashed line),  $T_W = 150$  GeV (red - dashed line) and  $T_W = 200$  GeV (green - long dashed line). The mass  $M$  grows to the right Left panel - normal hierarchy, right panel - inverted hierarchy.

asymmetry maximum is  $10^3$  times smaller than the estimate (C.1). This difference comes from the fact that one can not extremise both expressions in (C.2) at the same time for our choice of temperature. Let us take the case  $T = 100$  GeV for example. The maximum (for the inverted hierarchy) is reached for  $M = 25$  GeV,  $\epsilon = 0.5$  and  $\Delta M_M = 5 \cdot 10^{-12}$  GeV which extremises the first expression of (C.2), but the second is of  $O(10^{-3})$ . Looking at the analytical expression, we should decrease  $\Delta M_M$  and get more asymmetry, but we are already at the limit of validity of the perturbative expansion because of condition (iii) of Section 2.3.

## References

- [1] E. W. Kolb and M. S. Turner, *Grand Unified Theories and the Origin of the Baryon Asymmetry*, *Ann. Rev. Nucl. Part. Sci.* **33** (1983) 645–696.
- [2] S. Davidson, E. Nardi, and Y. Nir, *Leptogenesis*, *Phys. Rept.* **466** (2008) 105–177, [[arXiv:0802.2962](#)].
- [3] A. Pilaftsis, *Resonant tau leptogenesis with observable lepton number violation*, *Phys. Rev. Lett.* **95** (2005) 081602, [[hep-ph/0408103](#)].
- [4] A. Pilaftsis and T. E. J. Underwood, *Electroweak-scale resonant leptogenesis*, *Phys. Rev.* **D72** (2005) 113001, [[hep-ph/0506107](#)].
- [5] F. del Aguila, J. A. Aguilar-Saavedra, and R. Pittau, *Neutrino physics at large colliders*, *J. Phys. Conf. Ser.* **53** (2006) 506–527, [[hep-ph/0606198](#)].
- [6] S. Bray, J. S. Lee, and A. Pilaftsis, *Resonant CP violation due to heavy neutrinos at the LHC*, *Nucl. Phys.* **B786** (2007) 95–118, [[hep-ph/0702294](#)].
- [7] A. G. Cohen, D. B. Kaplan, and A. E. Nelson, *Progress in electroweak baryogenesis*, *Ann. Rev. Nucl. Part. Sci.* **43** (1993) 27–70, [[hep-ph/9302210](#)].
- [8] V. A. Rubakov and M. E. Shaposhnikov, *Electroweak baryon number non-conservation in the early universe and in high-energy collisions*, *Usp. Fiz. Nauk* **166** (1996) 493–537, [[hep-ph/9603208](#)].

- [9] M. Trodden, *Electroweak baryogenesis*, *Rev. Mod. Phys.* **71** (1999) 1463–1500, [[hep-ph/9803479](#)].
- [10] V. A. Kuzmin, V. A. Rubakov, and M. E. Shaposhnikov, *On the Anomalous Electroweak Baryon Number Nonconservation in the Early Universe*, *Phys. Lett.* **B155** (1985) 36.
- [11] M. E. Shaposhnikov, *Possible Appearance of the Baryon Asymmetry of the Universe in an Electroweak Theory*, *JETP Lett.* **44** (1986) 465–468.
- [12] M. E. Shaposhnikov, *Baryon Asymmetry of the Universe in Standard Electroweak Theory*, *Nucl. Phys.* **B287** (1987) 757–775.
- [13] M. Carena, G. Nardini, M. Quiros, and C. E. M. Wagner, *The Baryogenesis Window in the MSSM*, *Nucl. Phys.* **B812** (2009) 243–263, [[arXiv:0809.3760](#)].
- [14] D. J. H. Chung, B. Garbrecht, M. J. Ramsey-Musolf, and S. Tulin, *Yukawa Interactions and Supersymmetric Electroweak Baryogenesis*, *Phys. Rev. Lett.* **102** (2009) 061301, [[arXiv:0808.1144](#)].
- [15] T. Asaka, S. Blanchet, and M. Shaposhnikov, *The nuMSM, dark matter and neutrino masses*, *Phys. Lett.* **B631** (2005) 151–156, [[hep-ph/0503065](#)].
- [16] T. Asaka and M. Shaposhnikov, *The nuMSM, dark matter and baryon asymmetry of the universe*, *Phys. Lett.* **B620** (2005) 17–26, [[hep-ph/0505013](#)].
- [17] A. Boyarsky, O. Ruchayskiy, and M. Shaposhnikov, *The role of sterile neutrinos in cosmology and astrophysics*, *Ann. Rev. Nucl. Part. Sci.* **59** (2009) 191–214, [[arXiv:0901.0011](#)].
- [18] F. L. Bezrukov and M. Shaposhnikov, *The Standard Model Higgs boson as the inflaton*, *Phys. Lett.* **B659** (2008) 703–706, [[arXiv:0710.3755](#)].
- [19] M. Shaposhnikov and I. Tkachev, *The nuMSM, inflation, and dark matter*, *Phys. Lett.* **B639** (2006) 414–417, [[hep-ph/0604236](#)].
- [20] A. Kusenko, *Sterile neutrinos, dark matter, and the pulsar velocities in models with a Higgs singlet*, *Phys. Rev. Lett.* **97** (2006) 241301, [[hep-ph/0609081](#)].
- [21] A. Anisimov, Y. Bartocci, and F. L. Bezrukov, *Inflaton mass in the  $\nu$ MSM inflation*, *Phys. Lett.* **B671** (2009) 211–215, [[arXiv:0809.1097](#)].
- [22] F. Bezrukov and D. Gorbunov, *Light inflaton Hunter’s Guide*, *JHEP* **05** (2010) 010, [[arXiv:0912.0390](#)].
- [23] F. Bezrukov, D. Gorbunov, and M. Shaposhnikov, *On initial conditions for the Hot Big Bang*, *JCAP* **0906** (2009) 029, [[arXiv:0812.3622](#)].
- [24] A. Boyarsky, A. Neronov, O. Ruchayskiy, and M. Shaposhnikov, *The masses of active neutrinos in the nuMSM from X-ray astronomy*, *JETP Lett.* **83** (2006) 133–135, [[hep-ph/0601098](#)].
- [25] D. Gorbunov and M. Shaposhnikov, *How to find neutral leptons of the nuMSM?*, *JHEP* **10** (2007) 015, [[arXiv:0705.1729](#)].
- [26] E. K. Akhmedov, V. A. Rubakov, and A. Y. Smirnov, *Baryogenesis via neutrino oscillations*, *Phys. Rev. Lett.* **81** (1998) 1359–1362, [[hep-ph/9803255](#)].
- [27] M. Shaposhnikov, *The nuMSM, leptonic asymmetries, and properties of singlet fermions*, *JHEP* **08** (2008) 008, [[arXiv:0804.4542](#)].

- [28] A. Strumia and F. Vissani, *Neutrino masses and mixings and...*, [hep-ph/0606054](#).
- [29] A. D. Dolgov, *Neutrinos in the Early Universe*, *Sov. J. Nucl. Phys.* **33** (1981) 700–706.
- [30] R. Barbieri and A. Dolgov, *Neutrino oscillations in the early universe*, *Nucl. Phys.* **B349** (1991) 743–753.
- [31] G. Sigl and G. Raffelt, *General kinetic description of relativistic mixed neutrinos*, *Nucl. Phys.* **B406** (1993) 423–451.
- [32] B. Dasgupta, A. Dighe, G. G. Raffelt, and A. Y. Smirnov, *Multiple Spectral Splits of Supernova Neutrinos*, *Phys. Rev. Lett.* **103** (2009) 051105, [[arXiv:0904.3542](#)].
- [33] H. Duan, G. M. Fuller, and Y.-Z. Qian, *Collective Neutrino Oscillations*, [arXiv:1001.2799](#).
- [34] Y. Burnier, M. Laine, and M. Shaposhnikov, *Baryon and lepton number violation rates across the electroweak crossover*, *JCAP* **0602** (2006) 007, [[hep-ph/0511246](#)].
- [35] T. Asaka and H. Ishida, *Flavour Mixing of Neutrinos and Baryon Asymmetry of the Universe*, [arXiv:1004.5491](#).
- [36] **WA66** Collaboration, A. M. Cooper-Sarkar *et. al.*, *Search for Heavy Neutrino Decays in the BEBC Beam Dump Experiment*, *Phys. Lett.* **B160** (1985) 207.
- [37] **CHARM** Collaboration, F. Bergsma *et. al.*, *A Search for Decays of Heavy Neutrinos in the Mass Range 0.5-GeV to 2.8-GeV*, *Phys. Lett.* **B166** (1986) 473.
- [38] **NuTeV** Collaboration, A. Vaitaitis *et. al.*, *Search for neutral heavy leptons in a high-energy neutrino beam*, *Phys. Rev. Lett.* **83** (1999) 4943–4946, [[hep-ex/9908011](#)].
- [39] G. Bernardi *et. al.*, *Search for Neutrino Decay*, *Phys. Lett.* **B166** (1986) 479.
- [40] G. Bernardi *et. al.*, *Further Limits on Heavy Neutrino Couplings*, *Phys. Lett.* **B203** (1988) 332.
- [41] A. Atre, T. Han, S. Pascoli, and B. Zhang, *The Search for Heavy Majorana Neutrinos*, *JHEP* **05** (2009) 030, [[arXiv:0901.3589](#)].
- [42] **NuSOng** Collaboration, T. Adams *et. al.*, *Terascale Physics Opportunities at a High Statistics, High Energy Neutrino Scattering Experiment: NuSOng*, *Int. J. Mod. Phys.* **A24** (2009) 671–717, [[arXiv:0803.0354](#)].
- [43] S. R. Mishra, R. Petti, and C. Rosenfeld, *A High Resolution Neutrino Experiment in a Magnetic Field for Project-X at Fermilab*, *PoS Nufact08* (2008) 069, [[arXiv:0812.4527](#)].
- [44] G. R. Farrar and M. E. Shaposhnikov, *Baryon asymmetry of the universe in the standard electroweak theory*, *Phys. Rev.* **D50** (1994) 774, [[hep-ph/9305275](#)].